



**HAL**  
open science

# Fictitious domain for stabilization of fluid-structure interaction

Michel Fournié, Jonathan Morrison

► **To cite this version:**

Michel Fournié, Jonathan Morrison. Fictitious domain for stabilization of fluid-structure interaction. IFAC-PapersOnLine, 2017, 50 (1), pp.12301-12306. 10.1016/j.ifacol.2017.08.2478 . hal-01978052

**HAL Id: hal-01978052**

**<https://hal.science/hal-01978052>**

Submitted on 22 Jan 2019

**HAL** is a multi-disciplinary open access archive for the deposit and dissemination of scientific research documents, whether they are published or not. The documents may come from teaching and research institutions in France or abroad, or from public or private research centers.

L'archive ouverte pluridisciplinaire **HAL**, est destinée au dépôt et à la diffusion de documents scientifiques de niveau recherche, publiés ou non, émanant des établissements d'enseignement et de recherche français ou étrangers, des laboratoires publics ou privés.

# Fictitious domain for stabilization of fluid-structure interaction

Michel Fournié\* Jonathan Morrison\*\*

\* *Institut de Mathématiques, UMR 5219, Université Paul Sabatier  
Toulouse III, CNRS, 31062 Toulouse Cedex, France (e-mail:  
michel.fournie@math.univ-toulouse.fr).*

\*\* *Department of Aeronautics, Imperial College, London, South  
Kensington, SW7 2AZ, UK (e-mail: j.morrison@imperial.ac.uk).*

**Abstract:** We study the numerical approximation of the fluid structure interaction for stabilization of the fluid flow around an unstable stationary solution in a two dimensional domain, in the presence of boundary perturbations. We use a feedback control law recently proposed in [Airiau et al. (2017)] which is able to stabilize the nonlinear semi-discrete controlled system and based on the fluid only. Using Dirichlet boundary feedback, we deduce a boundary structure displacement. The fluid structure closed loop feedback is tested numerically using a fictitious domain finite element method based on extended Finite Element.

© 2017, IFAC (International Federation of Automatic Control) Hosting by Elsevier Ltd. All rights reserved.

*Keywords:* Control flow, Xfem, Fictitious domain, Adaptive Systems, Morphing Structures

## 1. INTRODUCTION

We study the numerical approximation of the fluid structure interaction stabilizing the fluid flow around an unstable stationary solution in a two dimensional domain, in the presence of boundary perturbations. The control is applied through a local deformation of the structure. The goal of the article is to propose a simple numerical feedback control based on the fluid flow using Dirichlet boundary condition and recently introduced in [Airiau et al. (2017)]. This feedback control is able to stabilize the nonlinear semi-discrete controlled system coming from a Finite Element approximation using conforming mesh refined around the structure. Such control corresponding to suction/blowing type was extensively studied in literature [He et al. (2000); Bergmann and Cordier (2008); Park et al. (1994)].

More recently, interests are focused on morphing control type. This concept suggests continuous adaptive deformations of the structure see [Ndiaye (2016)] for control theory and [Dearing et al. (2010); Garland et al. (2015)] for practical issue. In the present work, we propose a new strategy to define such feedback control (based on fluid only) to deduce the structure displacement. Numerical experiments require particular attention to match the motion of the structure into the fluid. This difficulty is address using fictitious domain approach based on extended finite element method (see [Court and Fournié (2015)]) which is interesting for the closed loop system. In particular, no numerical instability is introduced with some risks to destabilize the flow. The motivation of that work is to propose an efficient coupling that can be easily adapted to more complex models.

\* M. Fournié would like to thank ANR-Labex CIMI and RTRA-STAE-Foundation (Project DYNAMORPH) for their supports (sabbatical year at Imperial College).

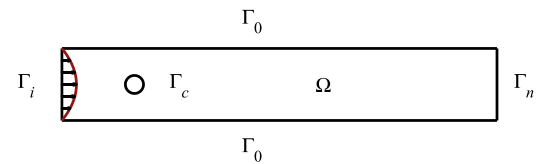


Fig. 1. Geometric configuration.

The outline of the paper is as follows. In Section 1, we define the feedback control issue from the fluid. In Section 2, the fictitious domain method is introduced. Next in Section 3, we present the closed loop algorithm coupling fluid and structure. Finally, in Section 4, we perform simulations and the conclusion is given in Section 5.

## 2. FLUID CONTROL STRATEGY

The geometrical domain is a rectangular channel  $\Omega = \mathcal{F} \cup \mathcal{S}$  where  $\mathcal{F}$  stands for the fluid domain and  $\mathcal{S}$  for the structure (modeled by a disk), see Fig. 1. We consider the case where the boundary  $\Gamma = \Gamma_d \cup \Gamma_n$ ,  $\Gamma_d$  is the part of  $\Gamma$  where Dirichlet boundary conditions are prescribed,  $\Gamma_n$  is the part of  $\Gamma$  where Neumann boundary conditions are prescribed and  $\Gamma_c$  corresponds to the boundary of the disk included into  $\Gamma_d$ .

The fluid is modeled by the Navier-Stokes equations

$$\begin{aligned} \frac{\partial w}{\partial t} + (w \cdot \nabla)w - \operatorname{div} \sigma(w, q) &= 0, \quad \operatorname{div} w = 0 \quad \text{in } Q_\infty, \\ w &= u_s + v_c + v_d \quad \text{on } \Sigma_d^\infty = \Gamma_d \times (0, \infty), \\ \sigma(w, q)n &= 0 \quad \text{on } \Sigma_n^\infty = \Gamma_n \times (0, \infty), \\ w(0) &= w_s \quad \text{on } \mathcal{F}, \end{aligned} \tag{1}$$

where  $Q_\infty = \mathcal{F} \times (0, \infty)$ ,  $\sigma(w, q) = 2\nu D(w) - qI$  is the Cauchy stress tensor with  $D(w) = \frac{1}{2}(\nabla w + (\nabla w)^T)$ ,  $\nu > 0$  is the kinematic viscosity of the fluid,  $w$  denotes the fluid velocity,  $q$  the fluid pressure,  $w_s$  is the stationary

velocity (coming from  $(w_s, q_s)$  the unstable solution of the stationary Navier-Stokes equations),  $v_c$  is the control function with support in  $\Gamma_c \times (0, \infty) \subset \Sigma_d^\infty$ ,  $u_s$  is supported in  $\Gamma_i \subset \Gamma_d$ , and  $v_d$  is a time dependent disturbance, with support in  $\Gamma_i \times (0, \infty)$ . We choose  $v_c$  of the form

$$v_c(x, t) = \sum_{i=1}^{N_c} v_i(t) g_i(x). \quad (2)$$

The functions  $g_i$  are the supports of the actuators, their location can be chosen in specific control zone  $\Gamma_c$  to improve the efficiency of the control (see [Airiau et al. (2017)] for the characterization of the *best control location*). The function  $v = (v_i)_{1 \leq i \leq N_c}$  is the control variable. Setting  $z = w - w_s$  and  $p = q - q_s$ , the nonlinear system satisfied by  $(z, p)$  is

$$\begin{aligned} \frac{\partial z}{\partial t} + (w_s \cdot \nabla)z + (z \cdot \nabla)w_s + (z \cdot \nabla)z - \operatorname{div} \sigma(z, p) &= 0, \\ \operatorname{div} z &= 0 \quad \text{in } Q_\infty, \quad z = v_c + v_d \quad \text{on } \Sigma_d^\infty, \\ \sigma(z, p)n &= 0 \quad \text{on } \Sigma_n^\infty, \quad z(0) = z_0 \quad \text{on } \mathcal{F}, \end{aligned} \quad (3)$$

while the linearized system is

$$\begin{aligned} \frac{\partial z}{\partial t} + (w_s \cdot \nabla)z + (z \cdot \nabla)w_s - \operatorname{div} \sigma(z, p) &= 0, \\ \operatorname{div} z &= 0 \quad \text{in } Q_\infty, \quad z = v_c + v_d \quad \text{on } \Sigma_d^\infty, \\ \sigma(z, p)n &= 0 \quad \text{on } \Sigma_n^\infty, \quad z(0) = z_0 \quad \text{on } \mathcal{F}. \end{aligned} \quad (4)$$

### 2.1 Semi-discrete approximation and control strategy

When we approximate systems (3) and (4) by a finite element method, the nonhomogeneous Dirichlet boundary conditions are taken into account in weak form by adding a Lagrange multiplier  $\tau(t)$ . We introduce finite dimensional subspaces  $X_h \subset H_{\Gamma_{o,i}}^1(\mathcal{F}; \mathbb{R}^2)$  for the velocity,  $M_h \subset L^2(\mathcal{F})$  for the pressure, and  $S_h \subset H^{-1/2}(\Gamma_d; \mathbb{R}^2)$  for the multipliers. We denote by  $(\phi_i)_{1 \leq i \leq N_z}$  a basis of  $X_h$ ,  $(\psi_i)_{1 \leq i \leq N_p}$  a basis of  $M_h$ , and  $(\zeta_i)_{1 \leq i \leq N_\tau}$  a basis of  $S_h$ , so

$$z = \sum_{i=1}^{N_z} z_i \phi_i, \quad p = \sum_{i=1}^{N_p} p_i \psi_i, \quad \tau = \sum_{i=1}^{N_\tau} \tau_i \zeta_i, \quad z_0 = \sum_{i=1}^{N_z} z_{0,i} \phi_i, \quad g_i = \sum_{k=1}^{N_\tau} g_k^i \zeta_k. \quad (5)$$

To simplify the writing of the semi-discrete model, it is convenient to concatenate the two Lagrange multipliers  $\mathbf{p}(t)$  (the discrete approximation of the pressure) and  $\tau(t)$  into the vector  $\boldsymbol{\eta} = (\eta_1, \dots, \eta_{N_\eta})^T = (p_1, \dots, p_{N_p}, \tau_1, \dots, \tau_{N_\tau})^T$ . If we denote by boldface letters the coordinate vectors, and  $N_\eta = N_p + N_\tau$ , we have  $\mathbf{z} = (z_1, \dots, z_{N_z})^T$ ,  $\mathbf{p} = (p_1, \dots, p_{N_p})^T$ ,  $\boldsymbol{\tau} = (\tau_1, \dots, \tau_{N_\tau})^T$ ,  $\mathbf{v} = (v_1, \dots, v_{N_c})^T$ ,  $\mathbf{z}_0 = (z_{0,1}, \dots, z_{0,N_z})^T$ . When  $v_d = 0$  (to simplify the presentation), the finite dimensional approximation of system (4) corresponds to

find  $z \in H_{\text{loc}}^1([0, \infty); X_h)$ ,  $p \in L_{\text{loc}}^2([0, \infty); M_h)$ , and  $\tau \in L_{\text{loc}}^2([0, \infty); S_h)$  such that,  $\forall \phi \in X_h$

$$\begin{aligned} \frac{d}{dt} \int_{\mathcal{F}} z(t) \phi \, dx &= a(z(t), \phi) + b(\phi, p(t)) + \langle \tau(t), \phi \rangle_{\Gamma_c}, \\ b(z(t), \psi) &= 0, \quad \forall \psi \in M_h, \end{aligned}$$

$$\langle \zeta, z(t) \rangle_{\Gamma_d} = \sum_{i=1}^{N_c} v_i(t) \langle \zeta, g_i \rangle_{\Gamma_c}, \quad \forall \zeta \in S_h \text{ where} \quad (6)$$

$$\begin{aligned} a(z, \phi) &= - \int_{\mathcal{F}} \left( \frac{\nu}{2} (\nabla z + (\nabla z)^T) : (\nabla \phi + (\nabla \phi)^T) + \right. \\ &\quad \left. ((w_s \cdot \nabla)z + (z \cdot \nabla)w_s) \phi \right) dx, \\ \text{and } b(\phi, p) &= \int_{\mathcal{F}} \operatorname{div} \phi p \, dx. \end{aligned}$$

We introduce the stiffness matrices  $A_{zz} \in \mathbb{R}^{N_z \times N_z}$ ,  $A_{zp} \in \mathbb{R}^{N_z \times N_p}$ ,  $A_{z\tau} \in \mathbb{R}^{N_z \times N_\tau}$ ,  $A_{z\eta} \in \mathbb{R}^{N_z \times N_\eta}$ , the mass matrices  $M_{zz} \in \mathbb{R}^{N_z \times N_z}$ ,  $M_{\tau\tau} \in \mathbb{R}^{N_\tau \times N_\tau}$ ,  $M_{\eta\eta} \in \mathbb{R}^{N_\eta \times N_\eta}$ , and the matrix  $\mathbf{G} \in \mathbb{R}^{N_\tau \times N_c}$  defined by  $(A_{zz})_{ij} = a(\phi_j, \phi_i)$ ,  $(A_{zp})_{ij} = b(\phi_i, \psi_j)$ ,  $(A_{z\tau})_{ij} = \langle \zeta_j, \phi_i \rangle_{\Gamma_c}$ ,  $A_{z\eta} = [A_{zp} \ A_{z\tau}]$ ,

$(M_{zz})_{ij} = (\phi_i, \phi_j)$ ,  $(M_{\tau\tau})_{ij} = \langle \zeta_i, \zeta_j \rangle_{\Gamma_c}$ ,  $M_{\eta\eta} = \begin{bmatrix} 0 \\ M_{\tau\tau} \end{bmatrix}$ , and  $\mathbf{G}$  is the matrix whose columns are the coordinate vectors of the actuators  $g_i$ . We recall that  $N_\eta = N_p + N_\tau < N_z$  and that  $A_{z\eta}$  is of rank  $N_\eta$ , so we have

$$\begin{bmatrix} M_{zz} & 0 & 0 \\ 0 & 0 & 0 \\ 0 & 0 & 0 \end{bmatrix} \begin{bmatrix} z' \\ p' \\ \tau' \end{bmatrix} = \begin{bmatrix} A_{zz} & A_{zp} & A_{z\tau} \\ A_{z\eta}^T & 0 & 0 \\ A_{z\eta}^T & 0 & 0 \end{bmatrix} \begin{bmatrix} z \\ p \\ \tau \end{bmatrix} - \begin{bmatrix} 0 \\ 0 \\ M_{\tau\tau} \mathbf{G} v \end{bmatrix}. \quad (7)$$

The two main difficulties to treat this problem are to deal with nonhomogeneous boundary conditions when the normal component of the Dirichlet boundary control is not zero, and to deal with a controlled system of large dimension (limitation to solve Riccati equation). To address these difficulties, we introduce  $\mathbf{\Pi}$  the discrete Leray projector of the system and project the dynamical system onto a space of small dimension. The system (7) is written into the form

$$\begin{aligned} M_{zz} \mathbf{z}'(t) &= A_{zz} \mathbf{z}(t) + A_{z\eta} \boldsymbol{\eta}(t), \quad \mathbf{\Pi}^T \mathbf{z}(0) = \mathbf{\Pi}^T \mathbf{z}_0, \\ 0 &= A_{z\eta}^T \mathbf{z}(t) - M_{\eta\eta} \mathbf{G} \mathbf{v}(t). \end{aligned} \quad (8)$$

We call the result proved in [Airiau et al. (2017)],  $(\mathbf{z}, \boldsymbol{\eta})$  is the solution of (8) if and only if it is the solution to

$$\begin{aligned} \mathbf{\Pi}^T \mathbf{z}'(t) &= \mathbf{A} \mathbf{\Pi}^T \mathbf{z}(t) + \mathbf{B} \mathbf{v}(t), \quad \mathbf{\Pi}^T \mathbf{z}(0) = \mathbf{\Pi}^T \mathbf{z}_0, \\ (I - \mathbf{\Pi}^T) \mathbf{z}(t) &= M_{zz}^{-1} A_{z\eta} (A_{z\eta}^T M_{zz}^{-1} A_{z\eta})^{-1} M_{\eta\eta} \mathbf{G} \mathbf{v}(t), \\ \boldsymbol{\eta}(t) &= (A_{z\eta}^T M_{zz}^{-1} A_{z\eta})^{-1} A_{z\eta}^T \mathbf{z}'(t) - \\ &\quad (A_{z\eta}^T M_{zz}^{-1} A_{z\eta})^{-1} A_{z\eta}^T M_{zz}^{-1} A_{zz} \mathbf{z}(t), \end{aligned} \quad (9)$$

where the infinitesimal generator  $\mathbf{A}$  and the control operator  $\mathbf{B}$  of the controlled system are defined by

$$\mathbf{A} = \mathbf{\Pi}^T M_{zz}^{-1} A_{zz} \text{ and}$$

$$\mathbf{B} = \mathbf{\Pi} A_{zz} M_{zz}^{-1} A_{z\eta} (A_{z\eta}^T M_{zz}^{-1} A_{z\eta})^{-1} M_{\eta\eta} \mathbf{G}.$$

Thus, we have determined the pair  $(\mathbf{A}, \mathbf{B})$  which is needed for control strategy of the linearized system (8) (or (9)). The family  $(g_i)_{1 \leq i \leq N_c}$  can be chosen in such a way that the pair  $(\mathbf{A}, \mathbf{B})$  is stabilizable in  $\operatorname{Ker}(A_{z\eta}^T)$ .

### 2.2 The projected dynamical system

By using the real Jordan decomposition of  $\mathbf{A} \mathbf{\Pi}^T$  we have

$$\Lambda = \mathbf{E}^{-1} \mathbf{A} \mathbf{\Pi}^T \mathbf{E} \text{ with } \Lambda = \begin{pmatrix} \Lambda_r & \mathbf{0}_{\mathbb{R}^{(N_z-d_\ell) \times d_\ell}} \\ \mathbf{0}_{\mathbb{R}^{d_\ell \times (N_z-d_\ell)}} & \mathbf{0}_{\mathbb{R}^{d_\ell \times d_\ell}} \end{pmatrix},$$

where  $d_\ell$  is the dimension of  $\operatorname{Ker}(\mathbf{A} \mathbf{\Pi}^T)$  and  $\Lambda_r \in \mathbb{R}^{(N_z-d_\ell) \times (N_z-d_\ell)}$  is invertible and is constituted of real Jordan blocks associated with the eigenvalues of  $\mathbf{A} \mathbf{\Pi}^T$

with real parts different from zero. The matrix  $\mathbf{E} \in \mathbb{R}^{N_z \times N_z}$  may be decomposed into the form  $\mathbf{E} = [\mathbf{E}_r \ \mathbf{E}_\ell]$  with  $\mathbf{E}_r \in \mathbb{R}^{N_z \times (N_z - d_\ell)}$  and  $\mathbf{E}_\ell \in \mathbb{R}^{N_z \times d_\ell}$ , and the columns of  $\mathbf{E}_\ell$  generate  $\text{Ker}(\mathbf{A}\mathbf{\Pi}^T)$ . In particular, for a given  $\mathbf{\Pi}^T \mathbf{z}$ , there is a unique  $\boldsymbol{\zeta}$  such that  $\mathbf{\Pi}^T \mathbf{z} = \mathbf{E}_r \boldsymbol{\zeta}$  and  $(9)_1$  is equivalent to an equation of the form

$$\boldsymbol{\zeta}'(t) = \Lambda_r \boldsymbol{\zeta}(t) + \mathbb{B} \mathbf{v}(t), \quad \boldsymbol{\zeta}(0) = \boldsymbol{\zeta}_0, \quad (10)$$

where  $\mathbb{B} = \mathbb{B}_s + \mathbb{B}_u$ ,  $\mathbb{B}_s$  and  $\mathbb{B}_u$  are defined in (13). Due to the definition of  $\mathbf{\Pi}^T$ , we have  $\mathbb{R}^{N_z} = \text{Ker}(A_{z\eta}^T) \oplus \text{Ker}(\mathbf{A}\mathbf{\Pi}^T)$ , and  $\text{Ker}(A_{z\eta}^T) = \oplus_{\lambda_j \neq 0, \text{Im}\lambda_j \geq 0} G_{\mathbb{R}}(\lambda_j)$ , where  $G_{\mathbb{R}}(\lambda_j)$  is the real generalized eigenspace associated with  $\lambda_j \in \text{spect}(\mathbf{A}\mathbf{\Pi}^T)$  (for the spectrum). We choose a family  $(\lambda_j)_{j \in J_u}$  containing all the unstable eigenvalues (with nonnegative imaginary part) of  $\mathbf{A}\mathbf{\Pi}^T$ . For the direct eigenvalue problem, we set

$$\mathbb{Z}_u = \oplus_{j \in J_u} G_{\mathbb{R}}(\lambda_j) = \text{vect}\{\mathbf{e}^1, \dots, \mathbf{e}^{d_u}\},$$

and for the adjoint eigenvalue problem, we set

$$\mathbb{Z}_u^* = \oplus_{j \in J_u} G_{\mathbb{R}}^*(\lambda_j) = \text{vect}\{\boldsymbol{\xi}^1, \dots, \boldsymbol{\xi}^{d_u}\}.$$

Thus, we have a decomposition of  $\text{Ker}A_{z\eta}^T$  of the form

$$\text{Ker}(A_{z\eta}^T) = \mathbb{Z}_u \oplus \mathbb{Z}_s \quad \text{with} \quad \mathbf{A}\mathbb{Z}_u \subset \mathbb{Z}_u \quad \text{and} \quad \mathbf{A}\mathbb{Z}_s \subset \mathbb{Z}_s, \quad (11)$$

and  $\mathbf{A}|_{\mathbb{Z}_s}$  is exponentially stable.

We denote by  $\mathbf{E}_u \in \mathbb{R}^{N_z \times d_u}$  the matrix whose columns are  $(\mathbf{e}^1, \dots, \mathbf{e}^{d_u})$ , and  $\boldsymbol{\Xi}_u$  the matrix whose columns are  $(\boldsymbol{\xi}^1, \dots, \boldsymbol{\xi}^{d_u})$ , then we have

$$\Lambda_u = \boldsymbol{\Xi}_u^T A_{zz} \mathbf{E}_u. \quad (12)$$

We also need the matrices of the Lagrange multipliers associated to the different families of eigenvectors introduced above. For that, we set  $\boldsymbol{\Xi}_{\eta,u} = \begin{pmatrix} \boldsymbol{\Xi}_{p,u} \\ \boldsymbol{\Xi}_{\tau,u} \end{pmatrix} \in \mathbb{R}^{N_\eta \times d_u}$  the matrix whose columns are  $(\boldsymbol{\eta}\boldsymbol{\xi}^1, \dots, \boldsymbol{\eta}\boldsymbol{\xi}^{d_u})$ .

Projecting the system (10) onto  $\mathbb{Z}_u$ , we have

$$\boldsymbol{\zeta}'_u(t) = \Lambda_u \boldsymbol{\zeta}_u(t) + \mathbb{B}_u \mathbf{v}(t), \quad \boldsymbol{\zeta}_u(0) = \boldsymbol{\Xi}_u^T M_{zz} \mathbf{z}_0, \quad (13)$$

with  $\mathbb{B}_u = -\boldsymbol{\Xi}_{\tau,u}^T M_{\tau\tau} \mathbf{G}$ . ( $\mathbb{B}_s$  can be defined similarly by projection onto  $\mathbb{Z}_s$ ).

To stabilize system (9), it is sufficient to stabilize (13) the equation satisfied by  $\boldsymbol{\zeta}_u$  and then to define a stabilizing feedback law  $\mathbb{K}_u$  using the solution  $\mathbb{P}_{\omega,u}$  of an algebraic Riccati equation. More precisely, for  $-\omega < \text{Re}(\Lambda_u)$ , the following algebraic Riccati equation

$$\begin{aligned} \mathbb{P}_{\omega,u} &\in \mathcal{L}(\mathbb{R}^{d_u}), \quad \mathbb{P}_{\omega,u} = \mathbb{P}_{\omega,u}^T \geq 0, \\ \Lambda_u + \omega I_{\mathbb{R}^{d_u}} - \mathbb{B}_u \mathbb{B}_u^T \mathbb{P}_{\omega,u} &\text{ is stable,} \\ \mathbb{P}_{\omega,u} (\Lambda_u + \omega I_{\mathbb{R}^{d_u}}) + (\Lambda_u^T + \omega I_{\mathbb{R}^{d_u}}) \mathbb{P}_{\omega,u} - \mathbb{P}_{\omega,u} \mathbb{B}_u \mathbb{B}_u^T \mathbb{P}_{\omega,u} &= 0, \end{aligned} \quad (14)$$

admits a unique solution  $\mathbb{P}_{\omega,u}$  and we define

$$\mathbb{K}_u = -\mathbb{B}_u^T \mathbb{P}_{\omega,u} \boldsymbol{\Xi}_u^T M_{zz}. \quad (15)$$

The closed loop linear system

$$\begin{aligned} M_{zz} \mathbf{z}'(t) &= A_{zz} \mathbf{z}(t) + A_{z\eta} \boldsymbol{\eta}(t), \\ \mathbf{z}(0) &= \mathbf{\Pi}^T \mathbf{z}_0 + M_{zz}^{-1} A_{z\eta} (A_{z\eta}^T M_{zz}^{-1} A_{z\eta})^{-1} M_{\eta\eta} \mathbf{G} \mathbb{K}_u \mathbf{z}_0, \\ A_{z\eta}^T \mathbf{z}(t) &= M_{\eta\eta} \mathbf{G} \mathbb{K}_u \mathbf{z}(t), \end{aligned} \quad (16)$$

is exponentially stable (with decay rate governed by the shift parameter  $\omega$ ).

Finally, the same linear feedback law  $\mathbb{K}_u$  is used in the nonlinear system (stabilizability can be proved using fixed point argument).

### 3. FICTITIOUS DOMAIN APPROACH

For the numerical procedure to solve Fluid Structure Interaction, a partitioned approach based on fictitious domain is retained.

#### 3.1 Extended Finite Element method with stabilization terms

The fictitious domain for the fluid is considered on the whole domain  $\Omega = \mathcal{F} \cup \mathcal{S}$ . Let us introduce three discrete finite element spaces  $\tilde{X}_h \subset H_{\Gamma_{o,i}}^1(\Omega)$  for the velocity,  $\tilde{M}_h \subset L^2(\Omega)$  for the pressure, and  $\tilde{S}_h \subset H^{-1/2}(\Gamma_d)$  for the multipliers. On the full domain  $\Omega$ , we consider a mesh  $\mathcal{T}^h$  with  $h = \max_{T \in \mathcal{T}^h} (h_T)$ ,  $h_T$  been the diameter of  $T$ . Finite element discretizations can be defined on the spaces  $\tilde{X}_h$ ,  $\tilde{M}_h$  and  $\tilde{S}_h$ . In order to separate the fluid domain and the structure domain, we define spaces on the fluid part  $\mathcal{F}$  and on the interface  $\Gamma_s$  only, as

$$X_h := \tilde{X}_h|_{\mathcal{F}}, \quad M_h := \tilde{M}_h|_{\mathcal{F}}, \quad S_h := \tilde{S}_h|_{\Gamma_s}.$$

Notice that  $X_h$ ,  $M_h$ ,  $S_h$  are respective natural discretizations spaces defined on the whole domain  $\Omega$  except where the basis functions are cutted by the structure. In that case, eXtended Finite Element Method (Xfem) is used. The standard finite element method basis functions  $(\phi_i)$ ,  $(\psi_i)$ ,  $(\zeta_i)$  defined in (5) are multiplied by Heaviside functions ( $H(\mathbf{x}) = 1$  for  $\mathbf{x} \in \mathcal{F}$  and  $H(\mathbf{x}) = 0$  for  $\mathbf{x} \in \mathcal{S}$ ), and the products are substituted in the variational formulation of the problem. This strategy presents several advantages in practice, however the order of convergence presents numerical locking and stabilization must be introduced to recover optimal convergence (see [Court and Fournié (2015)] for Navier-Stokes problems). Applying Xfem strategy with such penalization to the linearized Navier-Stokes equation (7) we obtain

$$\begin{bmatrix} M_{zz} & 0 & 0 \\ 0 & 0 & 0 \\ 0 & 0 & 0 \end{bmatrix} \begin{bmatrix} z' \\ p' \\ \tau' \end{bmatrix} = \begin{bmatrix} A_{zz} + A_{zz}^\gamma & A_{zp} + A_{zp}^\gamma & A_{z\tau} + A_{z\tau}^\gamma \\ A_{zp}^T + A_{zp}^{\gamma T} & A_{pp}^\gamma & A_{p\tau}^\gamma \\ A_{z\tau}^T + A_{z\tau}^{\gamma T} & A_{p\tau}^{\gamma T} & A_{\tau\tau}^\gamma \end{bmatrix} \begin{bmatrix} z \\ p \\ \tau \end{bmatrix} - \begin{bmatrix} 0 \\ 0 \\ M_{\tau\tau} \mathbf{G} v \end{bmatrix}, \quad (17)$$

where matrices indexed with  $\gamma$  are the contributions of stabilization terms issue from the following bilinear forms defined for  $z \in H_{\text{loc}}^1([0, \infty); X_h)$ ,  $p \in L_{\text{loc}}^2([0, \infty); M_h)$ ,  $\tau \in L_{\text{loc}}^2([0, \infty); S_h)$ , and  $\phi \in X_h$ ,  $\psi \in M_h$ ,  $\zeta \in S_h$ , by  $\mathcal{A}_{zz}^\gamma(z, \phi) = -4\nu^2 \gamma \int_{\Gamma} (D(z)n) \cdot (D(\phi)n) \, d\Gamma$ ,  $\mathcal{A}_{zp}^\gamma(\phi, p) = 2\nu\gamma \int_{\Gamma} p (D(\phi)n \cdot n) \, d\Gamma$ ,  $\mathcal{A}_{z\tau}^\gamma(z, \tau) = 2\nu\gamma \int_{\Gamma} \tau \cdot (D(z)n) \, d\Gamma$ ,  $\mathcal{A}_{pp}^\gamma(p, \psi) = -\gamma \int_{\Gamma} p \psi \, d\Gamma$ ,  $\mathcal{A}_{p\tau}^\gamma(\psi, \tau) = -\gamma \int_{\Gamma} \psi \tau \cdot n \, d\Gamma$ ,  $\mathcal{A}_{\tau\tau}^\gamma(\tau, \zeta) = -\gamma \int_{\Gamma} \tau \cdot \zeta \, d\Gamma$ .

#### 3.2 Extension to Navier-Stokes problem

To consider the time evolution with time step  $dt$  and to have unconditional stability of the scheme, we consider an implicit discretization based on the backward Euler

method. Newton algorithm is used to address the non-linearity. Particular attention must be done for a moving particle problem. Indeed, at the time level  $t^{n+1}$  the solid occupies  $\mathcal{S}(t^{n+1})$  which is different from the previous time level  $t^n$ . So, the field variable at the time level  $t^{n+1}$  can become undefined near the interface since there was no fluid flow at the time level  $t^n$  ( $\mathcal{S}(t^{n+1}) \neq \mathcal{S}(t^n)$  for the solid and  $\mathcal{F}(t^{n+1}) \neq \mathcal{F}(t^n)$  for the fluid). In other words, some degrees of freedom for the fluid part which are not considered at the time level  $t^n$  must be taken into account at the time level  $t^{n+1}$ , see Fig. 2. The velocity in that points is estimated by simple interpolation based on the velocity at the interface which is known at each time level. The location of the interface is governed by level-set.

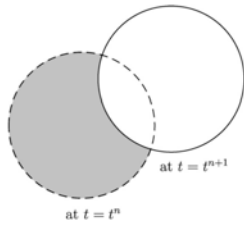


Fig. 2. Field variables in the shaded region are undefined at time  $t^{n+1}$ .

#### 4. CONTROL FOR FLUID STRUCTURE MODEL

One classical approach (used to obtain stabilization results) is the employment of change variables to overcome the difficulties introduced by the time dependence of the computational domain see [Ndiaye (2016)]. The feedback is then applied on one reference configuration (using a conforming mesh) and well defined at any time. However, this strategy is CPU-time consuming (extra terms to consider) and strongly dependent on the geometrical transformation. In the present work, we propose a new alternative based on the tools presented above (no transformation, non-conforming mesh).

On the hypothesis that the deformation of the structure is imposed which is a realistic hypothesis, we want to define a control under feedback form to govern this deformation. One useful example is a normal deformation (displacement) of two boundary zones (symmetric) and located in  $I_{\theta_q} = [\theta_q - 5^\circ, \theta_q + 5^\circ]$  for  $q = 1, 2$  (aperture  $\omega_q = 10^\circ$ ) (see Fig. 3). One deformation in one zone is characterized by one scalar  $d_q$  that corresponds to a displacement equal to  $d_q g_q^\theta(\vartheta)$  (with  $n$  unitary outward normal at the boundary)

$$g_q^\theta(\vartheta) = g\left(\frac{\vartheta + (-1)^q \theta}{\theta_a} + \frac{1}{2}\right) n(r_c \cos(\vartheta), r_c \sin(\vartheta)) \text{ for } q=1,2,$$

$$g(s) = G(10s) - G(10(s-1) + 1),$$

$$G(s) = s^3(6s^2 - 15s + 10) \text{ for } s \in ]0, 1[ \text{ and } G(s) = 0 \text{ elsewhere.} \quad (18)$$



Fig. 3. Location structure deformation at  $\theta = \pm 95^\circ$ .

The numerical procedure to solve these FSI problems is a partitioned approach that treats the fluid and the structure as two computational fields.

The interfacial conditions (continuity of the velocity between the fluid and the structure) are used explicitly to communicate information between the fluid and structure solutions. Motivation of this approach is to integrate available disciplinary algorithms (for fluid and structure) and reduce the code development time.

In order to propose a simple control strategy based on this partitioned approach, we consider the feedback  $\mathbb{K}_u$  in (15) based on the fluid velocity defined on  $\mathcal{F}(0)$  (considering no displacement of the structure,  $\mathcal{F}$  being fixed). The feedback computed only once allows to determine the velocity  $\mathbf{v}_c$  in (2) on  $I_{\theta_q}$  using (15) by

$$\mathbf{v}_c^n = \mathbb{K}_u(\mathbf{w}^0 - \mathbf{w}_s).$$

The feedback  $\mathbb{K}_u$  being defined on  $\mathcal{F}(0)$ , it can not be apply when structure deformation is introduced. Indeed, for FSI interaction,  $\mathcal{F}(t)$  depends on time. To overcome this difficulty (without using reference configuration),

- we extend by 0 the stationary solution  $w_s$  defined on  $\mathcal{F}(0)$  the full domain  $\Omega$  (so  $\mathbf{w}_s = 0$  on  $\mathcal{S}(0)$ )
- according to the time, we define two zones where the deformation acting,  $\Omega_d(t) = \{\mathcal{F}(t) \setminus \mathcal{F}(0)\} \cup \{\mathcal{S}(t) \setminus \mathcal{S}(0)\}$
- finally, we define an auxiliary velocity  $\tilde{\mathbf{w}}$  by

$$\tilde{\mathbf{w}}^n = \begin{cases} \mathbf{w}_s & \text{in } \Omega_d(t^n), \\ \mathbf{w}^n & \text{on } \mathcal{F}(t^n) \setminus \Omega_d(t^n). \end{cases}$$

The auxiliary velocity  $\tilde{\mathbf{w}}$  presents the advantage to be well defined at any time on  $\mathcal{F}(0)$  where we can apply the feedback  $\mathbb{K}_u$  and then we can use

$$\mathbf{v}_c^n = \mathbb{K}_u(\tilde{\mathbf{w}}^n - \mathbf{w}_s).$$

Finally from this estimation, we deduce the displacement of the structure  $d_q$  by simple integration and update the geometry (level-set) accordantly.

This approach can be justified by the fact that the instability of our FSI model is managed by the fluid only (unstable eigenvalues come from fluid). Moreover, the effect of using  $\tilde{\mathbf{w}}$  is weighted by the fact that the measure of  $\Omega_d$  tends to 0 according to the time (depending on the choice of  $\omega$  in (14)).

##### 4.1 Closed loop algorithm

For the closed loop system, we suppose that we have access on  $\mathcal{F}(t^n)$  at the time level  $t^n$  to  $(d^n, w^n, q^n, \tau^n)$ , the displacement, the velocity, the pressure, the multiplier, respectively. Then we search to compute on  $\mathcal{F}(t^{n+1})$  at the time level  $t^{n+1}$  the solution  $(d^{n+1}, w^{n+1}, q^{n+1}, \tau^{n+1})$ . The vectors of unknowns are denoted by  $\mathbf{d}^{n+1}, \mathbf{U}^{n+1}, \mathbf{P}^{n+1}, \mathbf{L}^{n+1}$ .

- 1- **Newton algorithm.** The computational domain  $\mathcal{F}(t^n)$  is given by  $\mathbf{d}^n$ . We compute  $(\mathbf{U}^{n+1}, \mathbf{P}^{n+1}, \mathbf{L}^{n+1})$

$$M_{uu} \frac{\mathbf{U}^{n+1} - \mathbf{U}^n}{dt} + A_{uu} \mathbf{U}^{n+1} + N(\mathbf{U}^{n+1}) \mathbf{U}^{n+1} + A_{up} \mathbf{P}^{n+1} + A_{u\lambda} \mathbf{L}^{n+1} = \mathbf{F}^{n+1},$$

$$A_{up}^T \mathbf{U}^{n+1} + A_{pp} \mathbf{P}^{n+1} + A_{p\lambda} \mathbf{L}^{n+1} = 0,$$

$$A_{u\lambda}^T \mathbf{U}^{n+1} + A_{p\lambda}^T \mathbf{P}^{n+1} + A_{\lambda\lambda} \mathbf{L}^{n+1} = \mathbf{G}^n,$$

where  $N(\mathbf{U}^{n+1})\mathbf{U}^{n+1}$  is the nonlinear term and  $\mathbf{G}^n$  represents the velocity imposed on the boundary of the structure (on  $I_{\theta_q}$ ) at the time level  $t^n$  (explicit).

2- **Auxiliary velocity.** We define

$$\tilde{\mathbf{U}}^{n+1} = \begin{cases} \mathbf{U}_s \text{ on } \Omega_d(t^n), \\ \mathbf{U}^{n+1} \text{ on } \mathcal{F}(t^n) \setminus \Omega_d(t^n). \end{cases}$$

3- **Feedback control.** We compute  $\mathbf{C}^{n+1} \in \mathbb{R}^2$ .

$$\mathbb{K}_u(\tilde{\mathbf{U}}^{n+1} - \mathbf{U}_s) = \mathbf{C}^{n+1}.$$

4- **Motion of the structure.** We compute  $\mathbf{d}^{n+1} \in \mathbb{R}^2$

$$\mathbf{d}^{n+1} = \mathbf{d}^n + dt\mathbf{C}^{n+1}.$$

5- **Morphing.** Update the geometry to determine  $\mathcal{F}(t^{n+1})$  from  $\mathbf{d}^{n+1}$  (based on (18))

6- **Update the velocity.** We complete  $\mathbf{U}^{n+1}$  defined on  $\mathcal{F}(t^n)$  to  $\mathcal{F}(t^{n+1})$ . The solution on  $\mathcal{F}(t^n) \cap \mathcal{F}(t^{n+1})$  remains unchanged while a simple interpolation based on  $\mathbf{C}^n$  and  $\mathbf{C}^{n+1}$  is completed (where new nodes appear see Fig. 2).

### 5. NUMERICAL EXPERIMENTS

We consider the domain  $\Omega = [-0.5, 2.25] \times [0, 0.4]$  and the cylinder is centered at the point  $(0.25, 0.2)$  with a diameter  $D = 0.1$ . The parabolic inflow condition on  $\Gamma_i = \{-0.5\} \times [0, 0.4]$  is

$$u_s(-0.5, x_2) = (u_s^1, u_s^2)^T = \left( 6 \left( \frac{x_2}{0.4} \left( 1 - \frac{x_2}{0.4} \right) \right), 0 \right)^T.$$

We define a triangular mesh (approximately 10.000 nodes) with local refinement near the deformation zones ( $I_{\theta_q}$ ). In Fig. 4 we represent the immersed disk with refinement near the boundary of the disk and a zoom on  $I_{\theta_q}$ . The best choice of locations  $I_{\theta_q}$  are justified in [Airiau et al. (2017)] and are fixed to  $\theta = \pm 95^\circ$ . The refinements of the mesh are used to ensure accuracy for any position of the structure. Some points inside the disk are not used when Xfem algorithm turns.

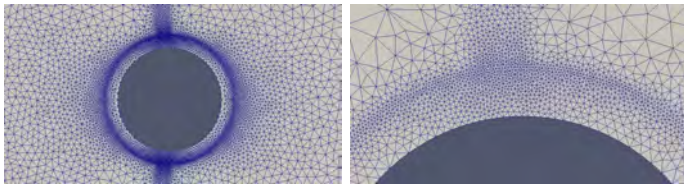


Fig. 4. The mesh with immersed disk.

The mesh is conform in the main part of the interface. When the deformation occurs on  $I_{\theta_q}$ , some elements are cut by the interface see Fig. 5.

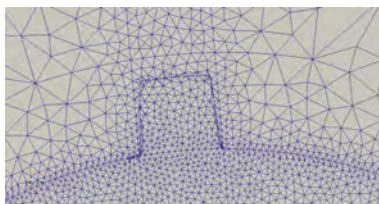


Fig. 5. Level-set to describe the displacement.

We use Taylor-Hood  $P_2-P_1-P_0$  finite element (with Xfem discretization) for the velocity, the pressure and the Lagrange multipliers respectively that brings to approximately 200000 degrees of freedom. The time step  $dt = 10^{-3}$  and  $Re = 100$ .

To define the feedback  $\mathbb{K}_u$ , for the linearized Navier-Stokes equation, we solve some eigenvalue problems using Arnoldi method with a 'shift and inverse' (ARPACK library) (a shift parameter fixed at 10 and a size of the small Hessenberg matrix equal to 400) see Fig. 6. As expected we have two unstable eigenvalues  $\lambda_1 = 2.344 \pm 17.542i$  ( $\lambda_2 = \bar{\lambda}_1$ ) that are used to define the reduced model (small Riccati (14)).

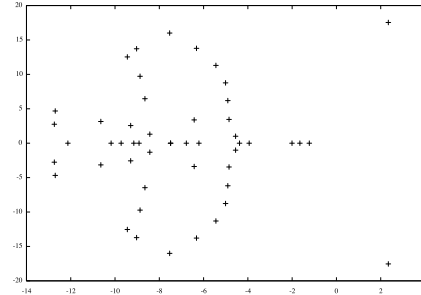


Fig. 6. Eigenvalues for  $Re = 100$  ( $Im(\lambda)$  versus  $Re(\lambda)$ ).

In order to test the efficiency of the feedback law, we introduce a boundary perturbation  $\mu(t)h(x)$  in the inflow boundary  $\Gamma_i \times (0, \infty)$ , localized in time (here  $t = 0$ ) and defined by  $f(t, x_2) = 0.375 e^{-30t^2} (\sigma(\xi_1, \mathbf{p}_{\xi_1}) \mathbf{n} \cdot \mathbf{n}, 0)^T$ , where  $\sigma(\xi_1, \mathbf{p}_{\xi_1}) \mathbf{n} \cdot \mathbf{n}$  (see Fig. 7) is the most destabilizing boundary perturbation (see [Airiau et al. (2017)] for more details).

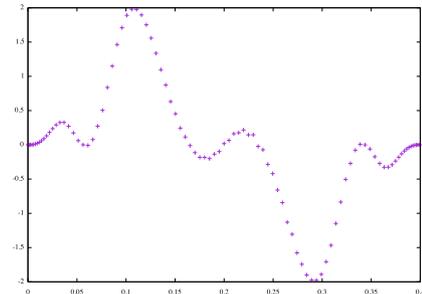


Fig. 7. Inflow perturbation ( $\sigma(\xi_1, \mathbf{p}_{\xi_1}) \mathbf{n} \cdot \mathbf{n}$  versus  $x_2$ ).

Such perturbation is approximately equal to 1/2 of the maximum value 3/2 of the inflow boundary condition. The perturbation is maximum at  $t = 0$  and the control is all the time applied. For  $Re = 100$ , it is well known that without control vortex street appears. In Fig. 8, we report the evolution of the control  $v_c$  corresponding to the velocity used to determine the deformation at the upper part of the disk (lower part is symmetric) and the evolution of the  $L^2$ -norm of the closed-loop solution  $\mathbf{z} = \mathbf{w} - \mathbf{w}_s$ .

In Fig. 9, we plot the evolution of the displacement for the upper part (lower part is symmetric). The maximum amplitude of the displacement is 0.0076 (for  $t = 0.059$ ) which corresponds to 7% of the diameter of the disk.

In Fig. 10, we report the velocity when the displacement is maximum and the streamlines at the same time (some recirculation near the bump on the upper part appears).

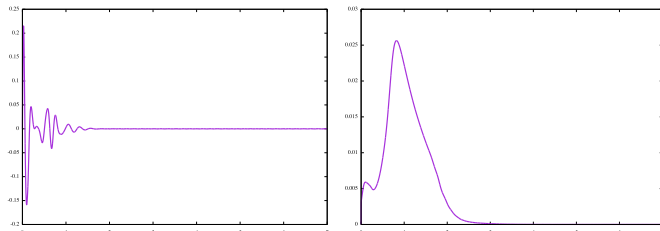


Fig. 8. Time evolution of the control  $\mathbf{v}_c$  and  $L^2$ -norm of  $\mathbf{z}$ .

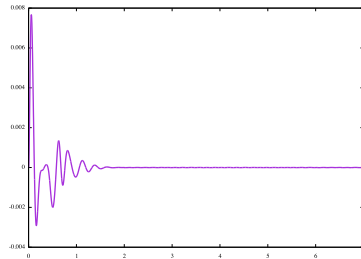


Fig. 9. Time evolution of the displacement (upper part).

Finally, we give some snapshots of the flow from the introduction of the perturbation in inflow to the state when the stationary velocity is recovered. Some illustrations of the level-set are superposed in Fig. 11.

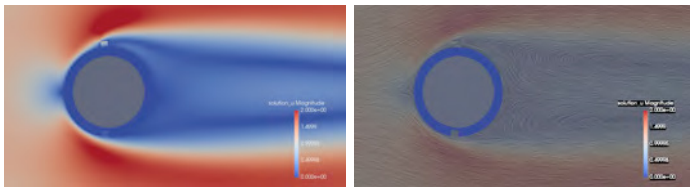


Fig. 10. Velocity magnitude and streamline at  $t = 0.07$ .

## 6. CONCLUSION

The feedback control based on fluid is sufficient to define the displacement of the structure able to stabilize the Fluid Structure Interaction model. The difficulty to define such control is widely simplified and classical numerical method can be used. The tools retained with fictitious domain are powerful and can be extended to other situations, like complex geometry in 2D and 3D or coupling with other structure models.

## REFERENCES

- Airiau, C., Buchot, J.M., Dubey, R., Fournié, M., Raymond, J.P., and Weller-Carlo, J. (2017). Stabilization and best actuator location for the navier-stokes equations. *In review, SIAM J. Sc. Comput.*
- Bergmann, M. and Cordier, L. (2008). Optimal control of the cylinder wake in the laminar regime by trust-region methods and pod reduced-order models. *J. Comput. Phys.*, 227, 7813–7840.
- Court, S. and Fournié, M. (2015). A fictitious domain finite element method for simulations of fluid-structure interactions: The navier-stokes equations coupled with a moving solid. *J. Fluids Struct.*, 55, 398–408.
- Dearing, S.S., Morrison, J.F., and Iannucci, L. (2010). Electro-active polymer (eap) dimple actuators for flow control: Design and characterisation. *Sensors and Actuators A: Physical*, 157(2), 210–218.

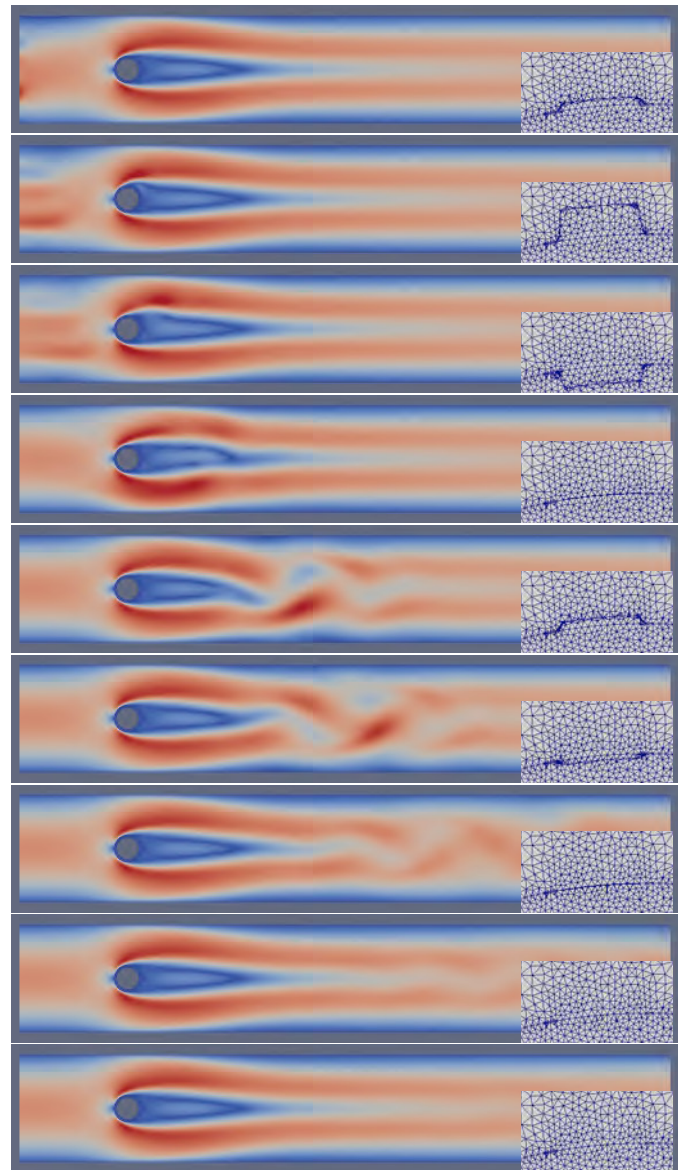


Fig. 11. Time evolution of the velocity magnitude for  $t = 10^{-3}, 0.1, 0.2, 0.4, 0.8, 1, 1.5, 2.0, 2.5$ .

- Garland, M., Santer, M.J., and Morrison, J.F. (2015). Adaptive vortex generator structures for the reduction of turbulent separation. *23rd AIAA/AHS Adaptive Structures Conference*, 1–11.
- He, J.W., Chevalier, M., Glowinski, R., Metcalfe, R., Nordlander, A., and Periaux, J. (2000). Drag reduction by active control for flow past cylinders. *Computational mathematics, Lecture Notes in Math.*, Springer, Berlin, 287–363.
- Ndiaye, M. (2016). Stabilization et simulation de modèles d'interaction fluide-structure. *PhD thesis, Université Paul Sabatier Toulouse III*.
- Park, D., D.M., L., and Hendricks, E. (1994). Feedback control of von karman vortex shedding behind a circular cylinder at low reynolds numbers. *Phys. Fluids*, 6, 2390–2405.